Articles

Probing the Dark State Tertiary Structure in the Cytoplasmic Domain of Rhodopsin: Proximities between Amino Acids Deduced from Spontaneous Disulfide Bond Formation between Cys316 and Engineered Cysteines in Cytoplasmic Loop 1[†,‡]

Judith Klein-Seetharaman,[§,∥] John Hwa,[§,⊥] Kewen Cai,[§,#] Christian Altenbach,[∇] Wayne L. Hubbell,[∇] and H. Gobind Khorana*,[§]

Massachusetts Institute of Technology, 77 Massachusetts Avenue, Cambridge, Massachusetts 02139, and Jules Stein Eye Institute and Department of Chemistry and Biochemistry, University of California, Los Angeles, California 90095

Received April 12, 2001; Revised Manuscript Received July 30, 2001

ABSTRACT: A dark state tertiary structure in the cytoplasmic domain of rhodopsin is presumed to be the key to the restriction of binding of transducin and rhodopsin kinase to rhodopsin. Upon light-activation, this tertiary structure undergoes a conformational change to form a new structure, which is recognized by the above proteins and signal transduction is initiated. In this and the following paper in this issue [Cai, K., Klein-Seetharaman, J., Altenbach, C., Hubbell, W. L., and Khorana, H. G. (2001) *Biochemistry 40*, 12479−12485], we probe the dark state cytoplasmic domain structure in rhodopsin by investigating proximity between amino acids in different regions of the cytoplasmic face. The approach uses engineered pairs of cysteines at predetermined positions, which are tested for spontaneous formation of disulfide bonds between them, indicative of proximity between the original amino acids. Focusing here on proximity between the native cysteine at position 316 and engineered cysteines at amino acid positions 55−75 in the cytoplasmic sequence connecting helices I−II, disulfide bond formation was studied under strictly defined conditions and plotted as a function of the position of the variable cysteines. An absolute maximum was observed for position 65 with two additional relative maxima for cysteines at positions 61 and 68. The observed disulfide bond formation rates correlate well with proximity of these residues found in the crystal structure of rhodopsin in the dark. Modeling of the engineered cysteines in the crystal structure indicates that small but significant motions are required for productive disulfide bond formation. During these motions, secondary structure elements are retained as indicated by the lack of disulfide bond formation in cysteines that do not face toward Cys316 in the crystal structure model. Such motions may be important in light-induced conformational changes.

Rhodopsin, the vertebrate dim-light photoreceptor, is a seven helical membrane protein that is prototypic for the largest known family of G-protein coupled receptors (*2*). It contains three distinct domains, the cytoplasmic (CP),[1] the transmembrane (TM), and the intradiscal (ID) domains. A molecule of 11-*cis*-retinal bound to Lys296 as a protonated Schiff base serves as a reverse agonist in the dark state. Light-catalyzed isomerization of the retinal to the all-trans form initiates movements in the TM helices (*3−5*), which bring about a conformational change in the tertiary structure in the CP domain. Subsequent interactions of transducin and rhodopsin kinase with the light-activated rhodopsin initiate visual signal transduction. Precise molecular description of the conformational change in rhodopsin induced by light and,
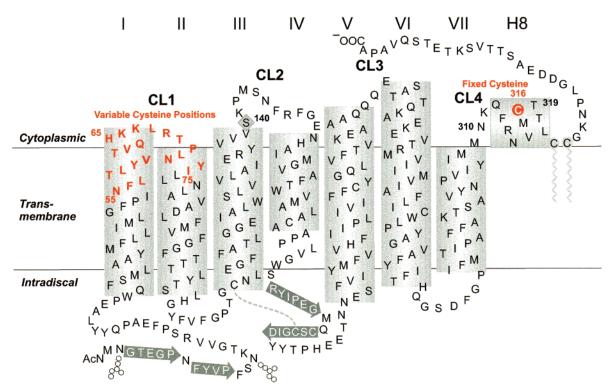
FIGURE 1: Secondary structure model based on the crystal structure of bovine rhodopsin (*15*) showing Cys316 and the positions of amino acids 55−75 in bold and red, replaced by cysteines one at a time. In all the 15 mutants containing cysteine pairs, Cys316 formed the fixed position. The native reactive Cys140 was replaced by serine (see text). TM helices are designated I−VII and CP loops CL1−CL4. The helix in CL4 observed in the crystal structure (*15*) is designated H8. β-Sheet structure is shown in dark gray.

Table 1: Sets of Cysteine Pairs Studied for Proximity Relationships in the Tertiary Structure of the CP Face of Rhodopsin

cysteine pairs		disulfide bond formed	
cysteine I (fixed)	cysteine II (varied)	most rapidly	reference
Cys316	Cys60 to Cys74	Cys65−Cys316	this work and ref *14*
Cys65	Cys306 to Cys321	Cys65−Cys316	*16*
Cys246	Cys311 to Cys314	Cys246−Cys312	*16*
Cys250	Cys311 to Cys314; Cys135	Cys250−Cys135	*16*
Cys139	Cys247 to Cys252	Cys139−Cys250; Cys139−Cys248[a]	*5*
Cys338	Cys240 to Cys250; Cys65; Cys140	Cys245−Cys338	*9*

[a] On the basis of EPR studies, these two cysteine pairs exhibited the strongest spin−spin interactions.

in GPCR in general upon ligand binding, is a long-range goal of studies on visual signal transduction.

Support for the presence of a dark state tertiary structure in the CP domain of rhodopsin in solution and its change on light-activation has been forthcoming from a series of previous studies. Single cysteine mutants spanning the entire CP face of rhodopsin were prepared and comprehensively studied for their biochemical effects on function (*6−10*) and for dark to light structural changes after spin labeling (*3, 4, 11−13*). As further probes of the tertiary structure, a large number of mutants containing pairs of cysteines at chosen sites in the CP domain were prepared and investigated for spontaneous formation of disulfide bonds as indicators of proximity between them (Figure 1, Table 1). For example, disulfide bond formation occurred rapidly in a mutant containing a cysteine at position 65 (in CL1) and the native Cys316 (in H8) (Figure 1) (*14*). Furthermore, disulfide bonds were observed in double cysteine mutants containing one cysteine fixed at position 139, CL2, and the second cysteine varied between position 248−251 in CL3 (*5*). Subsequently, proximity between Cys338 in the C-terminal polypeptide

chain and cysteine residues at positions Cys242 and Cys245 (CL3) was established by rapid disulfide bond formation (*9*).

Here, following the earlier finding of disulfide bond formation between cysteines at positions 65 and 316, we explore proximity between Cys316 and amino acids in the entire CL1. All the mutants containing cysteine pairs were generated by replacing amino acids, 55−75, one at a time by cysteine residues and retaining the native Cys316. The expressed proteins corresponding to the double cysteine mutants were all isolated in the sulfhydryl form and characterized. The spontaneous rates of disulfide bond formation were measured under constant conditions after increasing the pH to 7.7. The disulfide bond formation rate was at a maximum in the mutant containing Cys65 and Cys316, while two additional relative maxima were also observed for cysteines at positions 61 and 68. Comparison of the present results with the recently published three-dimensional model of rhodopsin derived from X-ray diffraction studies (*15*) shows an excellent correlation of the rates of disulfide bond formation with the actual distances between the original amino acids. The following paper in

this issue (*16*) further maps proximity between Cys65 and cysteines placed at positions 306–321 and between Cys246 or Cys250 and Cys311–314 (*16*) (Table 1).

MATERIALS AND METHODS

Unless stated otherwise, procedures were as described previously (*8*, *9*). 11-*cis*-Retinal was a gift from Rosalie Crouch (University of South Carolina of the National Eye Institute of the National Institutes of Health U.S. Public Health Services). The sulfhydryl reagent, 4,4′-dithiodpyridine (4-PDS), was purchased from Sigma (St. Louis, MO), and dodecylmaltoside (DM) was from Anatrace (Maumee, OH). Antirhodopsin monoclonal antibody 1D4 (*17*) was purified from a myeloma cell line provided by R. S. Molday (University of British Columbia). It was coupled to cyanogen bromide-activated Sepharose 4B (Sigma) as described (*17*). The nonapeptide (Massachusetts Institute of Technology Biopolymers Laboratory) corresponding to the C-terminal sequence of rhodopsin, the antibody epitope, was used to elute rhodopsin mutants from 1D4-Sepharose. Buffers used were buffer A, 137 mM NaCl, 2.7 mM KCl, 1.8 mM KH$_2$PO$_4$, 10 mM Na$_2$HPO$_4$ (pH 7.2); buffer B, buffer A plus 1% (wt/vol) DM, 2 mM ATP, 2 mM MgCl$_2$, and 0.1 mM phenylmethyanesulfonyl fluoride; buffer C, buffer A plus 0.05% DM (wt/vol); buffer D, 2 mM NaPi (pH 6.0), 0.05% DM (wt/vol); buffer E, 0.5 M Na$_2$PO$_4$, 0.05% DM; buffer F, 5 mM HEPES, pH 7.7, 0.05% DM.

Construction of Double Cysteine Rhodopsin Mutants. A mutant containing the C140S codon replacement has been constructed previously by Resek et al (*18*). All of the cysteine mutants (amino acids 55–75) were derivatives from this mutant except for H65C, which was constructed previously (*14*).

Mutants N55C, F56C, L57C, T58C, L59C, Y60C, V61C, T62C, V63C, Q64C, and K66C were prepared by fragment replacement mutagenesis in the synthetic gene for bovine opsin (*19*) in the expression vector PMT4 (*20*). DNA duplexes corresponding to the restriction fragments *Bcl*I/*Hin*dIII (nucleotides 147–205) containing all the cysteine substitution codons in the CL1 were used to replace the WT fragment. For mutants R69C, T70C, P71C, L72C, N73C, Y74C, and I75C, synthetic DNA duplexes cysteine substitution codons in CL1 corresponded to the restriction fragment *Hin*dIII/*Bgl*II (nucleotides 206–252).

A two-step technique was used for preparation of the mutant genes K67C and L68C. The first step involved PCR reactions with the WT plasmid as the template using the following primers containing the replaced cysteine codons: 5′GTCCAGCACAAGTGCCTTCGCACACCG-3′ for mutant K67C and the primer 5′-CCAGCACAAGAAGTGC-CGCACACCGCTC-3′ for mutant L68C. Details of the PCR reaction have been described previously (*21*). In the second step, the PCR products were all digested to give the corresponding small *Eco*RI/*Xho*I fragments (nucleotides 2–340) containing the cysteine substitution codons. These fragments were all subcloned into the large fragment *Xho*I/*Eco*RI (nucleotide 341–1061) of the parent plasmid containing the C140S substitution codon.

The DNA sequences of the fragments containing the replaced cysteine codons in each construct were confirmed by the dideoxynucleotide sequencing method (*22*).

Table 2: Characterization of Double Cysteine Substitution Mutants, N55C-I75C/Cys316

mutant	UV−vis absorption		Meta II decay $T_{1/2}$ (min)	no. of free sulfhydryl groups per rhodopsin
	λ_{max} (nm)	A_{280}/A_{500}		
WT	500	1.6	12.8	2
N55C/Cys316	496	2.0	5.5	1[a]
F56C/Cys316	499	1.6	9.9	1[a]
L57C/Cys316	499	1.6	10.7	1[a]
T58C/Cys316	499	1.6	9.8	1[a]
L59C/Cys316	499	1.7	12.5	1[a]
Y60C/Cys316	499	1.6	10.2	2
V61C/Cys316	499	1.7	11.2	2
T62C/Cys316	498	2.0	11.0	2
V63C/Cys316	499	1.7	11.6	2
N64C/Cys316	500	1.7	10.1	2
H65C/Cys316	499	1.7	11.0	2
K66C/Cys316	496	1.8	10.7	2
K67C/Cys316	498	1.9	11.2	2
L68C/Cys316	499	1.8	11.4	2
R96C/Cys316	498	1.7	11.2	2
T70C/Cys316	498	1.6	12.4	2
P71C/Cys316	498	2.0	9.7	2
L72C/Cys316	500	2.1	10.6	2
N73C/Cys316	499	2.0	10.0	2
T74C/Cys316	498	2.1	10.9	2
I75C/Cys316	500	1.6	9.8	1[a]

[a] The reactive cysteine in these mutants is Cys316. The second cysteine in CL1 was unreactive (see text and ref *8*).

Expression of the Mutant Opsin Genes and Purification of the Expressed Opsins after Reconstitution with 11-cis-Retinal. The mutant opsins expressed in COS-1 cells and reconstituted with 11-*cis*-retinal in buffer A (*17*) were solubilized in buffer B for 1 h at 4 °C in the dark. The suspensions were centrifuged at 124000*g* for 30 min at 4 °C and the supernates were incubated with appropriate amounts of the antibody 1D4-Sepharose beads as described (*17*). The resin was washed first with 30 bed volumes of buffer C, followed by a further wash with 15 bed volumes of buffer D. The protein was eluted with buffer D containing 70 μM epitope nonapeptide.

Determination of Rates of Disulfide Bond Formation. The rhodopsin double cysteine mutants after elution from 1D4-Sepharose were all diluted with buffer D to give 1.5 μM concentration, and the pH of the samples was then increased to 7.7 by the addition of buffer E. The time course of disulfide bond formation was monitored by taking aliquots (100 μL) at different time intervals and measuring the remaining free sulfhydryl content by reaction with 4-PDS in buffer F as described (*8*, *23*). The extent of disulfide bond formation for the double cysteine mutants was calculated from the decrease in the free sulfhydryl groups.

RESULTS

Characterization of the Rhodopsin Double Cysteine Mutants. (i) Spectral Characterization in the Dark. The double cysteine mutants, N55C-I75C/Cys316 (Figure 1) in the rhodopsin synthetic gene, were expressed in COS-1 cells and purified as described in Materials and Methods. All the mutants formed WT-like chromophores with λ_{max} at 498–500 nm and spectral ratios (A_{280}/A_{500}) of approximately 1.6–2.0 at pH 6 (Table 2). Interestingly, the extent of chromophore formation upon 11-*cis*-retinal binding of the mutant

with a N55C replacement alone was higher than that of the corresponding mutant with N55C/C140S/C316S triple replacement which formed chromophore poorly as reported previously (*8*).

(ii) Characterization of Light-Activation in the Mutants. Upon illumination, all mutants formed the characteristic Metarhodopsin II (Meta II) intermediate. As shown in Table 2, the $T_{1/2}$'s for decay of the latter, as measured by retinal release (*24*), were WT-like, ranging from 9.7 to 13.5 min^{-1} as compared to WT 12.8 min^{-1} under the conditions used. The mutant N55C/Cys316 is an exception with a particularly destabilized Meta II state ($T_{1/2}$, 5.5 min).

(iii) Cysteine Reactivity in the Mutants. To monitor disulfide bond formation, the loss of sulfhydryl-reactive groups in the mutants was followed with time. The concentration of free sulfhydryl groups was determined by reaction with 4-PDS, as described (*8, 23*). Native rhodopsin contains 10 cysteines, highlighted in Figure 1. Of these, only the two CP cysteines at positions 140 and 316 are reactive in the dark to the sulfhydryl derivatization reagent 4-PDS (*25*). In the present study, Cys140 was replaced by serine, leaving one reactive native cysteine at position 316. The cysteine pair mutants studied here should, therefore, show a derivatization stoichiometry of 2 per rhodopsin. As shown in Table 2, two cysteines per rhodopsin were found in double cysteine mutants Y60C-T74C/Cys316. However, in mutants N55C-L59C/Cys316 and I75C/Cys316, only one reactive sulfhydryl per rhodopsin was found with 4-PDS. This is consistent with the results of the previous study of the corresponding single cysteine mutants (*8*). Cysteines placed at positions 55−59 and at 75 were not reactive to 4-PDS, presumably because of being buried in the micelle environment and/or protein interior.

The validity of our indirect method of determining disulfide bond formation rates by means of determining the loss of free sulfhydryl groups depends on the assumption that the rate of the reaction of free sulfhydryl groups with 4-PDS is fast compared with the rates of disulfide bond formation. Preliminary experiments carried out at pH 7.2 showed that the $T_{1/2}$ of disulfide bond formation was on the order of tens of minutes to hours. However, the $T_{1/2}$ of the reaction of double cysteine mutant rhodopsins with 4-PDS was on the order of several minutes at this pH (data not shown). To determine conditions at which the $T_{1/2}$ of the reaction of cysteine mutants with 4-PDS was <1 min, it was necessary to measure the rate of reaction with 4-PDS as a function of pH for Cys316, the cysteine common to all double cysteine mutants.

The mutant rhodopsin with single reactive cysteine at position Cys316 was purified at pH 6. The pH was then adjusted to the approximate desired pH and the exact pH was then measured using a pH microelectrode. The rate of reaction with 4-PDS was plotted as a function of pH (Figure 2). The rates of reaction were constant below pH 6.8. However, as seen, between pH 7.3 and 7.7, the rate increased rapidly. Above pH 7.7, the rates of reaction with 4-PDS were constant, >80% complete by the time the first spectrophotometric measurement was performed (~1 min). Thus, disulfide bond formation was measured throughout at pH 7.7.

Disulfide Bond Formation in the Double Cysteine Mutants, N55C-I75C/Cys316, in the Dark. Before measuring disulfide
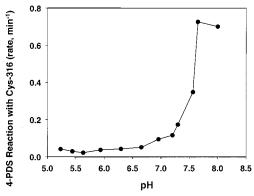

FIGURE 2: Reaction of Cys316 with 4-PDS as a function of pH. The rhodopsin mutant used contained C140S replacement.
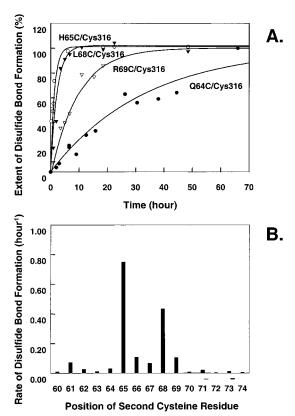

FIGURE 3: Disulfide bond formation in double cysteine mutants Y60C−Y74C/Cys316. Disulfide bond formation was measured at pH 7.7, 25 °C. (A) Time courses of disulfide bond formation between Cys316 and selected cysteines (at positions 64, 65, 68, 69) in CL1. (B) Plots of rates of disulfide bond formation between Cys316 and single cysteines in the mutants Y60C to T74C (Figure 1).

bond formation, the presence of two sulfhydryl groups was confirmed in all mutants Y60C-T74C at pH 6 (time zero). The rates of disulfide bonds formed as a function of time are shown in Figure 3A for selected mutants. The solid line in each case is the least-squares best fit of the data to apparent first order. From such fits, the apparent rate constant for each reaction was determined. Figure 3B shows these rates for double cysteine mutants Y60C−T74C/Cys316.

Disulfide bond formation was most rapid between Cys316 and H65C, followed closely by L68C. Cysteines at positions 66−69 and 61 also formed disulfide bonds, with half-reaction times of <10 h. Cysteines at 62 and 64 may also have formed disulfide bonds, but at a very small rate. In mutants with cysteine replacements at positions 60, 63, 70, 72−74, the

decrease in free sulfhydryl groups was insignificant, comparable to WT. The small decrease observed was likely due to protein aggregation and/or intermolecular disulfide bond formation as a consequence of prolonged incubation at 25 °C. A loss of sulfhydryl reactivity over extended periods of time has been observed earlier in studies with single cysteine mutants (unpublished observations). No disulfide bond formation was observed for cysteines at positions 55−59 and 75 (data not shown). In these mutants, instead of two free sulfhydryl groups only one free sulfhydryl group was present initially (see above), but the loss of reactivity over time was also insignificant. Thus, positions 55−60, 63, 70, and 72−75 did not appear to be in close proximity to Cys316. Closest proximity based on disulfide bond formation was to positions 65 and 68.

DISCUSSION

Naturally occurring disulfide bonds in folded proteins reflect their tertiary structure. Conversely, disulfide bond formation may be used to establish proximity between amino acids in folded protein domains where the tertiary structures are not known. Practical applications of disulfide bond formation in structural work were developed by Falke and Koshland (*26*) in studies of the aspartate receptor (*27, 28*).

Structural analysis of disulfides occurring in protein crystal structures showed that there are preferred conformations for their formation (*29*). The distance between α-carbon atoms across the disulfide ranges from about 4 to 9 Å in crystal structures, with 95% of all refined disulfides in the range 4.4 and 6.8 Å. The average distances across left-handed and right-handed disulfides is 5.88 ± 0.49 Å and 5.07 ± 0.73 Å (*30*), respectively. Thus, the presence of a disulfide bond indicates that the α-carbons of the participating cysteines are about 5−6 Å apart. However, the geometry derived from crystallography may not hold in solution, especially for mobile regions at protein surfaces (*30*). The formation of a disulfide bond between two cysteines does not imply a time-average proximity of the two residues in the protein structure. Once the disulfide bond is formed, the two cysteines are locked in the conformation that may not necessarily be favored.

Rates of disulfide bond formation are influenced by pK_as of the sulfhydryl groups in proteins, which can vary over several orders of magnitude (*30, 31*). Here, it was not feasible to take into account the different ionization constants for the sulfhydryl groups of cysteines at different positions in the CP face of rhodopsin. It is also possible that traces of metal ions were present that could serve as catalysts. However, as much as possible, efforts have been made to obtain comparative data on spontaneous disulfide bond formation. Therefore, all the experiments reported in this and the following paper in this issue (*16*) were carried out under identical conditions. At the start of the reactions, both cysteine groups participating in disulfide bond formation were quantitatively in their sulfhydryl form, as shown by titration of the cysteines with 4-PDS (see Results) and relative rates for disulfide bond formation between different cysteine pairs were measured. Within a similar range of mobilities and a similar environment, the relative differences in rates of disulfide bond formation should be primarily influenced by proximity.

Meaningful derivation of proximity between one cysteine and neighboring cysteines requires systematic variation of
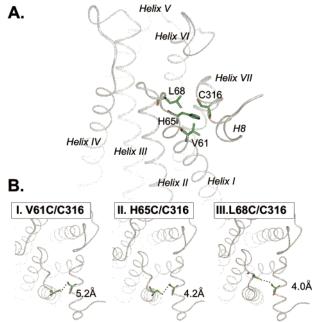

FIGURE 4: Proximity between Cys316 and His65, Leu68 and Val61. (A) Location of His65, Leu68 and Val61 in the crystal structure (*15*). On the basis of the ability to form disulfide bonds with Cys316 the fastest (Figure 3), cysteines placed at positions 65, 68, and 61 were deduced to be in closest proximity to Cys316. The positions of these residues in the crystal structure are shown here. (B) Replacement of residues by cysteines in the crystal structure model. Residues were mutated to cysteines using the InsightII software. The rotamer with least number of steric clashes and minimum energy was chosen. Then, the distance between sulfur atoms was determined. (I) H61C Replacement. (II) L65C Replacement. (III) L68C Replacement.

the neighboring sites. In the experiments reported, Cys316 was kept constant and the second cysteine was varied from position 55 to 75. Of the double cysteine pairs studied here, only very few formed disulfide bonds and the rates of disulfide bond formation varied with the position of the cysteine in CL1. Disulfide bond formation between Cys65 and Cys316 was most rapid, confirming the previous observation (*14*). In addition, disulfide bonds also formed rapidly between Cys316 and the cysteines at positions 68 and 61, followed by slow interaction with cysteines at positions 66−69. The small number of disulfide bonds formed and the large differences in rates of disulfide bond formation indicate that residues 65, 68, and 61 are relatively closer to Cys316 than the other sites studied and the cysteine at position 65 is oriented most suitably to form a disulfide bond.

Very recently, a three-dimensional structure model based on X-ray crystallographic analysis of rhodopsin has appeared (*15*). This enabled us to compare proximities between amino acids deduced from the above experiments with the crystallographic model. The position of Cys316 on one hand and of Val61, His65, and Leu68 on the other in the crystal structure (Figure 4A) indeed show close proximity. To compare proximity quantitatively in the crystal with that derived from the disulfide bond formation rates, the double cysteine replacements were introduced in the rhodopsin crystal structure using the InsightII program. The cysteine rotamer with the least steric interference and the minimum energy was chosen without any further adjustments in the structure surrounding the cysteine replacements. Then, the
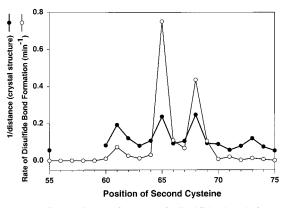
FIGURE 5: Comparison of rates of disulfide bond formation observed between Cys316 and cysteines at positions 55−75 in CL1 with S−S distances in the rhodopsin crystal structure. (○) Disulfide bond formation rates. (●) Reciprocal of distances from Sγ to Sγ of the two cysteines. Distances between sulfur atoms were determined as described in Figure 4.

distances between the sulfur atoms of Cys316 and every one of the cysteine replacements, positions 55 and 60−75, were measured. For the positions, 61, 65, and 68, forming rapid disulfide bonds, a view of the residues within the crystal structure is shown in Figure 4B, panels I−III, respectively. The reciprocal of all the distances obtained as a function of residue position and the rates of disulfide bond formation (from Figure 3B) are shown in Figure 5. The comparison showed excellent correlation between the rates of disulfide bond formation and the interthiol distances derived from the cysteine replacements in the crystal structure. The three positions that most rapidly formed disulfide bonds with Cys316, H65C, L68C, and V61C, are 4−5 Å distant from Cys316 (Figures 4 and 5). In order for a disulfide bond to form, however, 3−4 Å translational movements would be necessary. This requires that there be sufficient flexibility of the amino acids in this region of the rhodopsin CP face. The fact, however, that only those cysteines that faced Cys316 were able to bridge this small gap indicates that there is no unfolding of the ends of the helices, but rather a movement of intact helices which brings residues in CL1 close to Cys316.

The above conclusion of dynamical behavior of this region of the receptor is supported by EPR analysis of nitroxide labeled derivatives of the above double-cysteine mutants (Altenbach et al, unpublished results). Furthermore, NMR analysis of ^{15}N-lysine labeled rhodopsin suggests extensive conformational exchange on a microsecond to millisecond time scale (Klein-Seetharaman et al, unpublished results). While EPR and NMR parameters represent averages over a bulk population, disulfide cross-linking can occur by trapping rare events in backbone motions. This allows analysis of backbone dynamics over a large range of time scales (*26*, *32*). The rates of disulfide bond formation determined here demonstrate the existence of flexibility and time-dependent fluctuations in the tertiary structure in the rhodopsin CP domain of rhodopsin. Further support for the proposed structural fluctuations in this region comes from an analysis of the temperature factors reported for this region in the crystal structure of the rhodopsin dark-state dimer (*15*). This analysis is shown in Figure 6. First, the thermal factors are generally very high, and second, they are significantly different for the two halves of the dimer in the crystal. In
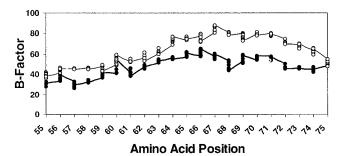

FIGURE 6: Temperature factors as a function of amino acid position in the region 55−75. The temperature factors were obtained from the rhodopsin crystal structure coordinate file 1F88 (*15*). Since rhodopsin was modeled as a dimer, two sets of temperature factors were reported and are plotted here.

both sets, temperature-factors values also vary with amino acid position indicating the presence of heterogeneity in mobility, but overall trends are quite similar within each set. However, the appearance of the temperature-factor spectrum over this range of amino acid positions 55−75 is very different from the observed rate pattern for disulfide bond formation. While a broad center of mobility was found in the temperature factor plot, with maximum mobility around residues 67−68, the rates of disulfide bond formation show distinct maxima, indicating that in this set of mutants, clearly proximity of residues dominated the pattern of disulfide bond formation.

The fluctuations indicated above may have functional significance. Light-induced conformational changes in this region have been observed qualitatively earlier (*8*, *10−12*). Furthermore, EPR analysis of nitroxide labeled derivatives of the double-cysteine mutants studied here revealed that light-activation of rhodopsin generally caused an increase in the distance between the nitroxides and in some cases an increase in the width of the distance distribution (Altenbach et al, unpublished results). Particularly, nitroxide residues at 62 and 65 on helix I and residue 73 on helix II showed increases in distances relative to Cys316. These residues are located at sites facing the inside of the helical bundle, i.e., facing helix VII. This suggests an outward movement of helix I and helix II away from H8, a motion that would result in opening a cleft in the helical bundle. Similarly, the motions required to produce disulfide cross-linking also indicate relative movements of helices I and II. Thus, the conformational flexibility in the dark may be a prerequisite for the corresponding light-induced motion.

ACKNOWLEDGMENT

REFERENCES

1. Loewen, M. C., Klein-Seetharaman, J., Getmanova, E. V., Reeves, P. J., Schwalbe, H. and Khorana, H. G. (2001) *Proc. Natl. Acad. Sci. U.S.A.* 98, 4888−4892.
2. Baldwin, J. M., Schertler, G. F. X., and Unger, V. M. (1997) *J. Mol. Biol.* 272, 144−164.
3. Farahbakhsh, Z. T., Ridge, K. D., Khorana, H. G., and Hubbell, W. L. (1995) *Biochemistry 34*, 8812−8819.

4. Altenbach, C., Yang, K., Farrens, D. L., Farahbakhsh, Z. T., Khorana, H. G., and Hubbell, W. L. (1996) *Biochemistry 35*, 12470−12478.

5. Farrens, D. L., Altenbach, C., Yang, K., Hubbell, W. L., and Khorana, H. G. (1996) *Science 274*, 768−770.

6. Yang, K., Farrens, D. L., Hubbell, W. L., and Khorana, H. G. (1996) *Biochemistry 35*, 12464−12469.

7. Ridge, K. D., Zhang, C., and Khorana, H. G. (1995) *Biochemistry 34*, 8804−8811.

8. Klein-Seetharaman, J., Hwa, J., Cai, K., Altenbach, C. A., Hubbell, W. L., and Khorana, H. G. (1999) *Biochemistry 38*, 7938−7944.

9. Cai, K., Langen, R., Hubbell, W. L., and Khorana, H. G. (1997) *Proc. Natl. Acad. Sci. U.S.A. 94*, 14267−14272.

10. Cai, K., Klein-Seetharaman, J., Farrens, D., Zhang, C., Altenbach, C., Hubbell, W. L., and Khorana, H. G. (1999) *Biochemistry 38*, 7925−7930.

11. Altenbach, C., Klein-Seetharaman, J., Hwa, J., Khorana, H. G., and Hubbell, W. L. (1999) *Biochemistry 38*, 7945−7949.

12. Altenbach, C., Cai, K., Khorana, H. G., and Hubbell, H. G. (1999) *Biochemistry 38*, 7931−7937.

13. Langen, R., Cai, K., Altenbach, C., Khorana, H. G., and Hubbell, W. L. (1999) *Biochemistry 38*, 7918−7924.

14. Yang, K., Farrens, D. L., Altenbach, C., Farahbakhsh, Z. T., Hubbell, W. L., and Khorana, H. G. (1996) *Biochemistry 35*, 14040−14046.

15. Palczewski, K., Kumasaka, T., Hori, T., Behnke, C. A., Motoshima, H., Fox, B. A., LeTrong, I., Teller, D. C., Okada, T., Stenkamp, R. E., Yamamoto, M., and Miyano, M. (2000) *Science 289*, 739−745.

16. Cai, K., Klein-Seetharaman, J., Altenbach, C., Hubbell, W. L., and Khorana, H. G. (2001) *Biochemistry 40*, 12479−12485.

17. Oprian, D. D., Molday, R. S., Kaufman, R. J., and Khorana, H. G. (1987) *Proc. Natl. Acad. Sci. U.S.A. 84*, 8874−8878.

18. Resek, J. F., Farahbakhsh, Z. T., Hubbell, W. L., and Khorana, H. G. (1993) *Biochemistry 32*, 12025−12032.

19. Ferretti, L., Karnik, S. S., Khorana, H. G., Nassal, M., and Oprian, D. D. (1986) *Proc. Natl. Acad. Sci. U.S.A. 83*, 599−603.

20. Franke, R. R., Sakmar, T. P., Oprian, D. D., and Khorana, H. G. (1988) *J. Biol. Chem. 263*, 2119−2122.

21. Hwa, J., Garriga, P., Liu, X., and Khorana, H. G. (1997) *Proc. Natl. Acad. Sci. U.S.A. 94*, 10571−10576.

22. Sanger, F., Nicklen, S., and Coulson, A. R. (1977) *Proc. Natl. Acad. Sci. U.S.A. 74*, 5463−5467.

23. Grassetti, D. R., and Murray, J. F., Jr. (1967) *Arch. Biophys. 119*, 41−49.

24. Farrens, D. L., and Khorana, H. G. (1995) *J. Biol. Chem. 270*, 5073−5076.

25. Chen, Y. S., and Hubbell, W. L. (1978) *Membr. Biochem. 1*, 107−130.

26. Falke, J. J., and Koshland, D. E. (1987) *Science 237*, 1596−600.

27. Falke, J. J., Dernburg, A. F., Sternberg, D. A., Zalkin, N., Milligan, D. L., and Koshland, D. E. J. (1988) *J. Biol. Chem. 263*, 14850−14858.

28. Milligan, D. L., and Koshland, D. E. J. (1988) *J. Biol. Chem. 263*, 6268−6275.

29. Richardson, J. S. (1981) *Adv. Protein Chem. 34*, 167−339.

30. Kosen, P. A. (1992) in *Stability of Protein Pharmaceuticals, Part A: Chemical and Physical Pathways of Protein Degradation* (Ahern, T. J., and Manning, M. C., Eds.) Plenum Press, New York.

31. Shaked, Z., Szajewski, R. P., and Whitesides, G. M. (1980) *Biochemistry 19*, 4156−4166.

32. Careaga, C. L., and Falke, J. J. (1992) *J Mol Biol. 226*, 1219−35.